RAPID COMMUNICATION

J Neurophysiol
88: 507–513, 2002; 10.1152/jn.00909.2001.

A Model of Spike-Timing Dependent Plasticity: One or Two Coincidence Detectors?

UMA R. KARMARKAR AND DEAN V. BUONOMANO
Departments of Neurobiology and Psychology, University of California, Los Angeles, California 90095-1761

Received 5 November 2001; accepted in final form 15 March 2002

Karmarkar, Uma R. and Dean V. Buonomano. A model of spike-timing dependent plasticity: one or two coincidence detectors? *J Neurophysiol* 88: 507–513, 2002; 10.1152/jn.00909.2001. In spike-timing dependent plasticity (STDP), synapses exhibit LTD or LTP depending on the order of activity in the presynaptic and postsynaptic cells. LTP occurs when a single presynaptic spike precedes a postsynaptic one (a positive interspike interval, or ISI), while the reverse order of activity (a negative ISI) produces LTD. A fundamental question is whether the "standard model" of plasticity in which moderate increases in Ca^{2+} influx through the *N*-methyl-D-aspartate (NMDA) channels induce LTD and large increases induce LTP, can account for the order and interval sensitivity of STDP. To examine this issue we developed a model that captures postsynaptic Ca^{2+} influx dynamics and the associativity of the NMDA receptors. While this model can generate both LTD and LTP, it predicts that LTD will be observed at both negative and positive ISIs. This is because longer and longer positive ISIs induce monotonically decreasing levels of Ca^{2+}, which eventually fall into the same range that produced LTD at negative ISIs. A second model that incorporated a second coincidence detector in addition to the NMDA receptor generated LTP at positive intervals and LTD only at negative ones. Our findings suggest that a single coincidence detector model based on the standard model of plasticity cannot account for order-specific STDP, and we predict that STDP requires two coincidence detectors.

INTRODUCTION

The temporal relationship between pre- and postsynaptic activity can determine the direction of plasticity in synapses from several brain areas (Bi and Poo 1998; Debanne et al. 1994, 1998; Feldman 2000; Levy and Steward 1983; Markram et al. 1997; Zhang et al. 1998). This spike-timing dependent plasticity (STDP) is sensitive to the order of and interspike interval (ISI) between action potentials. Specifically, repetitive presentation of a presynaptic spike followed by a postsynaptic spike induces long-term potentiation (LTP). Conversely, if the presynaptic spike succeeds the postsynaptic one, long-term depression (LTD) ensues. As depicted in the schematic in Fig. 1, the interval between the pre- and postsynaptic spikes modulates the degree of STDP. A sharp discontinuity is observed at 0 ms where differences of a few milliseconds can determine whether maximal LTP or LTD is induced (Bi and Poo 1998; Feldman 2000; Zhang et al. 1998).

Since STDP exhibits a LTD and an LTP component, it is reasonable to ask whether it is based on the same mechanisms as associative LTP and homosynaptic LTD. Associative LTP relies on *N*-methyl-D-aspartate receptors (NMDARs), which function as coincidence detectors of pre- and postsynaptic activity. A presynaptic spike results in the release of glutamate, which binds to the NMDAR. Depolarization caused by a postsynaptic spike then produces a voltage-dependent expulsion of Mg^{2+}. Only when these events occur in close temporal proximity will the NMDA channels allow the influx of Ca^{2+}. Since glutamate can remain bound to the NMDAR for tens of milliseconds, a postsynaptic spike occurring after a presynaptic one can result in Ca^{2+} influx. This is a plausible mechanism for spike-timing dependent potentiation, as both the interval and order sensitivity would arise in part from the properties of the NMDAR.

The mechanisms underlying the induction of homosynaptic LTD are more complex. While low-frequency stimulation (LFS) can produce an NMDAR-independent form of LTD that depends on metabotropic glutamate receptors (Oliet et al. 1997), LTD induced by LFS generally depends on NMDARs (Bear and Abraham 1996). NMDAR-dependent LTD can also be induced by pairing presynaptic stimulation with moderate depolarization that is thought to partially open NMDA channels (Cummings et al. 1996). These data are consistent with what will be referred to as the standard model of long-term plasticity, which holds that moderate levels of Ca^{2+} above baseline induce LTD while high levels cause LTP (Lisman 1989). It is not known whether these same NMDAR-based mechanisms can account for the order and interval sensitivity of the LTD component of STDP. Specifically, it is unclear why an NMDAR-based model would produce little or no LTD at long negative ISIs and maximal LTD at short ones. In both cases, the membrane of the postsynaptic cell should have returned to close to its resting potential before the release of glutamate from the presynaptic terminal.

To determine whether the standard model of long-term plasticity can account for the characteristics of STDP, we constructed a set of models that capture the fundamental properties of the NMDAR and of postsynaptic Ca^{2+} influx. The first of these models is based on the NMDAR as an associative molecule coupled with the assumptions of the standard model. The second involves the NMDAR and an additional coincidence detector that is primarily responsible for the timing sensitivity of LTD. Our results predict that a second coincidence detector is necessary to account for the temporal properties of STDP.

Address for reprint requests: D. V. Buonomano, Departments of Neurobiology and Psychology, University of California, Box 951763, Los Angeles, CA 90095 (E-mail: dbuono@ucla.edu).

The costs of publication of this article were defrayed in part by the payment of page charges. The article must therefore be hereby marked "*advertisement*" in accordance with 18 U.S.C. Section 1734 solely to indicate this fact.

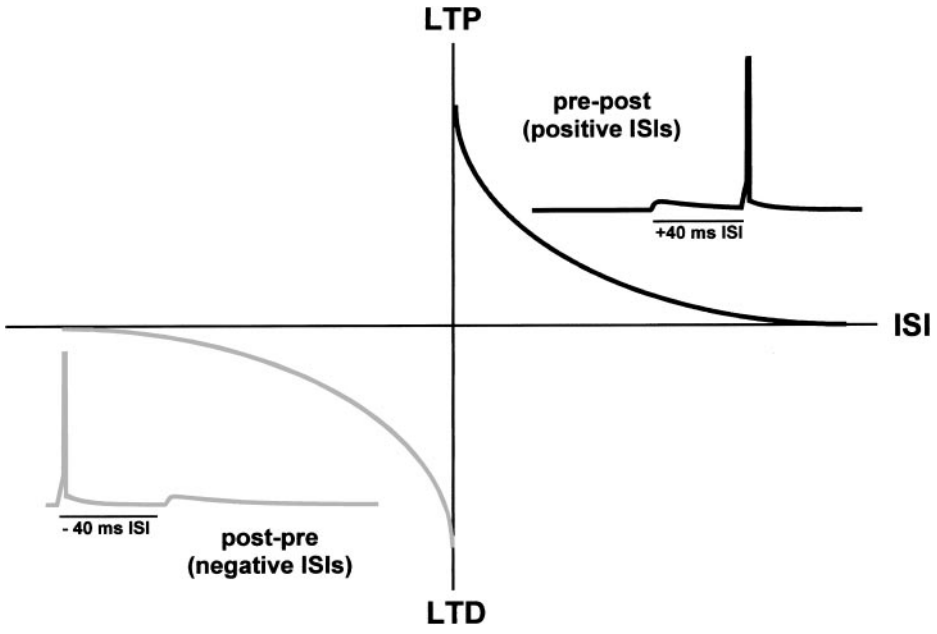

FIG. 1. Schematic of order-specific spike-timing dependent plasticity (STDP) function. Maximal plasticity is produced by short negative or positive interspike intervals (ISIs). Representative traces from the models of pairings at negative ISIs (*gray inset*) and positive ISIs (*black inset*).

METHODS

A presynaptic and postsynaptic cell were simulated; each cell was modeled as an integrate-and-fire unit. The E_{leak} was -60 mV, and spike threshold was set at -40 mV. Membrane voltage was reset to -56 mV after a spike. All simulations were conducted with the modeling program NEURON (Hines and Moore 1997).

Synaptic currents

The pre- and postsynaptic cells were connected by an excitatory synapse with both α-amino-3-hydroxy-5-methyl-4-isoxazolepropionic acid (AMPA) and NMDA receptors. The channel kinetics and synaptic currents were simulated as described previously (Buonomano 2000). The constants determining the binding (α) and dissociation (β) of glutamate to the postsynaptic receptors were based on the values in Buonomano (2000), Bekkers and Stevens (1993), and Lester and Jahr (1992), with the exception of the fast dissociation constant for NMDARs in *model 1* (see DISCUSSION), and are listed below

AMPA	NMDA
$\alpha = 0.5\ ms^{-1}$	$\alpha = 0.072\ ms^{-1}$
$\beta = 0.25\ ms^{-1}$	$\beta = 0.075\ ms^{-1}$ (*model 1*)
	$\beta = 0.025\ ms^{-1}$ (*model 1,2*)

Model 1

The first model simulates the peak total Ca^{2+} concentration of the postsynaptic terminal. This Ca^{2+} pool is fed by two sources with independent influx kinetics: one through voltage-gated Ca^{2+} channels (VGCCs), and the second through NMDA channels. The Ca^{2+} that enters the cell through the VGCCs ($VGCa^{2+}$) was modeled as a sigmoidal function dependent on the membrane voltage, with a decay time constant (τ) of 15 ms and a driving force of ($v - 140$) in the following equation

$$\frac{dVGCa}{dt} = [k_1(v - 140)\sigma(v)] - \frac{VGCa}{\tau} \quad (1)$$

where $k_1 = -0.023$ and the voltage-dependent channel kinetics were represented as $\sigma(v) = 1/[1 + \exp(-v + 0.1)]$.

The Ca^{2+} influx through the NMDA channels is dependent on the membrane voltage and presence of bound glutamate. The Mg^{2+} block of the NMDA channels is modeled as a sigmoidal voltage-dependent function: $B(v) = 1/\{1 + \exp[0.0868(-v - 10)]\}$, approximated from experimental data (Bekkers and Stevens 1993). The glutamate dependence is determined by the R_{NMDA} term, calculated as described in Buonomano (2000). The change in NMDAR Ca^{2+} entering the cell is calculated using these terms, the driving force, and the Ca^{2+} decay rate

$$\frac{dNMDACa}{dt} = \left\{-0.008(v - 140)\left[B(v)\frac{R_{NMDA}}{k_2}\right]\right\} - \frac{NMDACa}{\tau} \quad (2)$$

The results of this model were determined for two NMDAR dissociation constants (see Fig. 2*D*, results). When $\beta = 0.075$, $k_2 = 0.6178$, and for $\beta = 0.025$, $k_2 = 0.6792$.

To calculate Ca^{2+} as a function of ISI for this model, the results of the influx equations for $NMDACa^{2+}$ and $VGCa^{2+}$ were summed, and the maximum value of this sum, (Ca_{peak}) was recorded at each ISI. This value was also used to calculate plasticity. The equation describing plasticity (P) as a function of peak Ca^{2+}, as plotted in Fig. 2*C*, is represented as follows

$$P(Ca_{peak}) = 2.8\left[\frac{1}{1 + e^{4(-Ca_{peak} - k_3)}}\right] - 2\left[\frac{1}{1 + e^{12(-Ca_{peak} - k_4)}}\right] + 0.7858 \quad (3)$$

For calculation of the model using an NMDAR dissociation constant of $\beta = 0.075$: $k_3 = 0.2118$, $k_4 = 0.7128$, and for $\beta = 0.025$: $k_3 = 0.4534$, $k_4 = 0.9314$.

Model 2

The fundamental difference in this model is the addition of a second associative mechanism to account for LTD. Two separate Ca^{2+} sources act independently within the cell. Ca^{2+} influx through VGCCs is involved in the LTD pathway and Ca^{2+} from NMDA channels is involved in the induction of LTP. The equation for the VGCC opening kinetics, $\sigma(v)$, is identical to that for *model 1*. *Equation 1* is used again for $VGCa^{2+}$, with the scaling factor $k_1 = -0.019$. The coincidence detection in this pathway is determined by the simultaneous presence of both glutamate at the terminal (C), and Ca^{2+} from VGCCs. We will refer to the resulting associational value as mGlu (see DISCUSSION)

$$mGlu = VGCa * C \quad (4)$$

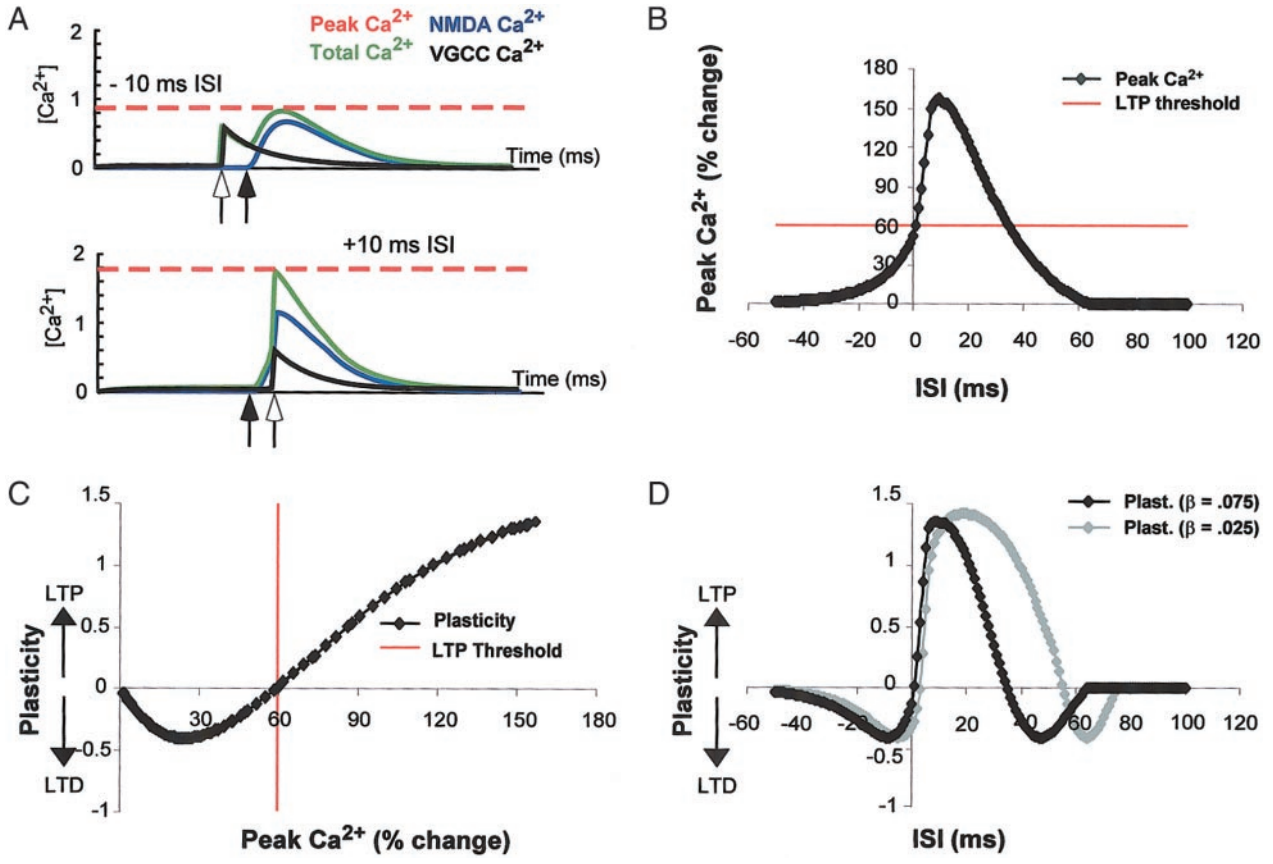

FIG. 2. *Model 1*, based on the standard model and a single coincidence detector. *A*: representative Ca^{2+} concentrations as computed in *model 1* for a −10-ms (*top*) and a +10-ms (*bottom*) ISI. The voltage-gated Ca^{2+} channel (VGCC) Ca^{2+} (black) and the *N*-methyl-D-aspartate receptor (NMDAR)–dependent Ca^{2+} (blue) are summed into a single pool (green). The peak Ca^{2+} influx (red) is measured from this sum and is used as the model output for each ISI. Filled arrows indicate excitatory postsynaptic potential (EPSP) onset; open arrows indicate postsynaptic spike onset. *B*: graph of percentage change in peak Ca^{2+} values for each ISI from −50 to +100. *C*: plot of plasticity as a function of percentage change in peak Ca^{2+}. *D*: STDP curve determined by applying the plasticity vs. Ca^{2+} function (*C*) to the model's Ca^{2+} output as a function of ISI (*B*). Black trace is determined from the values displayed in *C* and *B;* gray trace is the output of the same model with an alternate NMDAR dissociation constant ($\beta = 0.025$). Arbitrary units used for Ca^{2+} and plasticity measurements.

The model outputs the integral of this LTD coincidence detection value across each ISI. The integral's relationship to plasticity, once corrected for baseline, is directly proportional to that used as the measure of LTD. The possible contribution of $VGCa^{2+}$ to LTP is left undefined.

The $NMDACa^{2+}$ is determined by the following equation. The Mg^{2+} block equation, $B(v)$, and the glutamate-dependent term, R_{NMDA}, are calculated in the same manner as *model 1*

$$\frac{dNMDACa}{dt} = \left\{ -0.0105(v - 140)\left[B(v)\frac{R_{NMDA}}{0.6792}\right]^4 \right\} \quad (5)$$

The integral of this Ca^{2+} measure produces a value for the total NMDAR-dependent Ca^{2+} concentration in the soma across one pairing and is calculated at each ISI. Similarly to the $VGCa^{2+}$ activated pathway, this integral is used as the direct measure of plasticity, in this case LTP.

Induction protocol

Pairing was simulated by eliciting an action potential in each cell at ISIs ranging from −50 to +100 ms. ISIs were defined by the onset time of the first event to the onset time of the second event. For postsynaptic bursts the cell spiked three times at 20 Hz.

RESULTS

Model 1

The first model was based on the hypothesis that increases in Ca^{2+} above baseline account for both LTD (low Ca^{2+}) and LTP (high Ca^{2+}). To determine whether this standard model could at least in theory account for STDP, we optimized the model parameters toward this goal. Two important assumptions were made: the first that Ca^{2+} from the VGCCs and NMDA channels combines into a single pool; second, that the postsynaptic action potential exhibits an afterdepolarization that lasts on the order of tens of milliseconds (e.g., Fig. 3 in Feldman 2000). This slower positive voltage component of the spike serves as the record of postsynaptic activity.

Figure 2*A* represents the Ca^{2+} influx at ISIs of −10 ms (*top*) and +10 ms (*bottom*). The traces show the Ca^{2+} contributions from both channels as well as the peak total Ca^{2+} (red line) for each ISI. The peak Ca^{2+} level is significantly higher for the +10-ms interval due to both the NMDAR response to simultaneous binding of glutamate and depolarization (blue line) and the temporal summation of Ca^{2+} influx from VGCCs and NMDA channels (green line). The percentage change from baseline of peak Ca^{2+} values recorded for each ISI produce the

relationship depicted in Fig. 2*B*. There is an increase in Ca^{2+} concentration from negative to positive ISIs that declines again at long positive ISIs. If the Ca^{2+} pool is solely responsible for producing LTD at negative intervals as well as LTP at positive intervals, the model must be constrained so that the Ca^{2+} level at the 0-ms ISI is the LTD/LTP threshold. It is possible to design a function relating Ca^{2+} to plasticity that satisfies these requirements (Fig. 2*C*).

Combining the relationships in Fig. 2, *B* and *C*, results in the plasticity-ISI function shown in black in Fig. 2*D*. Although LTD and LTP are observed at the expected negative and positive intervals, respectively, LTD is also observed at long positive intervals. This is an important parameter-independent result of this model. For example, the entire model was recalculated after changing the NMDAR dissociation constant (β) from 0.075 to 0.025. The functional consequence of this change is that glutamate remains bound to the receptor for a longer period of time, allowing more Ca^{2+} to accumulate in the postsynaptic cell. This results in the relationship of plasticity to ISI represented in gray in Fig. 2*D*. Despite the changes in overall Ca^{2+} concentration that the altered parameter causes, the model still produces LTD at positive ISIs. This departure from the order specificity depicted in Fig. 1 is predictable from the plot of Ca^{2+} by ISI (Fig. 2*B*), which shows that the Ca^{2+} concentration at positive ISIs will eventually fall within the range that produces LTD.

Model 2

We next examined whether the STDP function illustrated in Fig. 1 can be simulated by adding a second coincidence detector. This model, like *model 1*, assumes that supralinear quantities of Ca^{2+} entering through the NMDA channels from an excitatory postsynaptic potential (EPSP) followed closely by an action potential cause LTP and its timing sensitivity. The timing of LTD, however, is determined through a second point of association that detects the interaction between a glutamate-activated pathway and the Ca^{2+} entering through the VGCCs due to the postsynaptic spike. Experimental data from acute hippocampal slices support a coincidence detection mechanism based on Ca^{2+}-dependent modulation of the metabotropic glutamate receptor (mGluR)–mediated pathway (Normann et al. 2000, see DISCUSSION). Based on this mechanism, at negative ISIs, voltage-gated Ca^{2+} would enter the postsynaptic cell first. Depending on the Ca^{2+} decay time and the length of the ISI, a certain concentration of Ca^{2+} would still be present when glutamate is released from the presynaptic terminal. The VGCC-based Ca^{2+} would then interact directly with the mGluR, or with a downstream element in the mGluR-activated pathway. Figure 3*A* plots Ca^{2+} activity by ISI and shows the two functionally distinct Ca^{2+} pools: Ca^{2+} entering through NMDA channels (black), and that which enters through VGCCs and interacts with the glutamate-dependent pathway (gray). At the negative ISIs, the LTD-inducing response depends on the amount of calcium from the VGCCs present at the time that the glutamate-dependent pathway is activated. The interval sensitivity of this response is derived from the Ca^{2+} decay rate.

Pre-post activity triggers the NMDA-based response that produces LTP, as described in *model 1*. Post-pre activity, however, induces functional changes through a separate mechanism, detecting Ca^{2+} from VGCCs rather than the NMDA receptor. Therefore in its simplest form, the mechanisms underlying LTD and LTP are independent in this model. The graph of the relationship of plasticity to ISI in Fig. 3*B* shows that the separate functions relating the two types of activity to potentiation and depression are assumed to be directly proportional to the values for postsynaptic Ca^{2+}-based activity. Most importantly, the model maintains order specificity and accounts for the sharp discontinuity between maximal depression and potentiation as the ISI approaches zero.

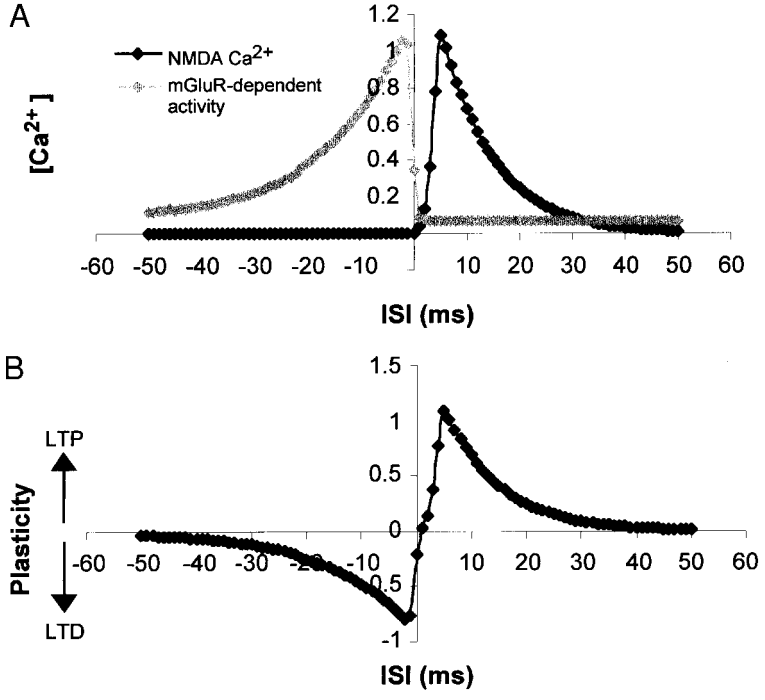

FIG. 3. *Model 2*, based on 2 coincidence detectors. *A*: the integral values for NMDAR Ca^{2+} influx (black) and mGluR-dependent pathway activity (gray) for a range of positive and negative ISIs. *B*: the complete STDP function produced by using the model output in (*A*) as a directly proportional measure of plasticity.

STDP using burst protocols

To determine how both models generalize to more physiological activity patterns, we paired a presynaptic spike with a burst of three postsynaptic spikes. Figure 4*A* shows the resulting Ca^{2+} to ISI relationship for *model 1*. Increasing the number of postsynaptic spikes increased the Ca^{2+} influx through the VGCCs, forcing the calcium concentration for all of the ISI points to fall well above the range for LTD. Since the type of plasticity in *model 1* is determined by a fixed threshold that relates to the Ca^{2+} levels produced by single spikes, the model is sensitive to increases in the degree of activity.

Figure 4*B* represents the responses from *model 2* when a protocol involving a postsynaptic burst was implemented. The shape of the plasticity-to-ISI function is similar to that of the original single spike simulation and maintains order sensitivity. The independence of the two pathways allows the two types of activity to scale without affecting the qualitative shape of the function. The response of *model 2* to increased activity is also well predicted by linear calculations from its original single-spike STDP function, as shown by the red curve (see DISCUSSION).

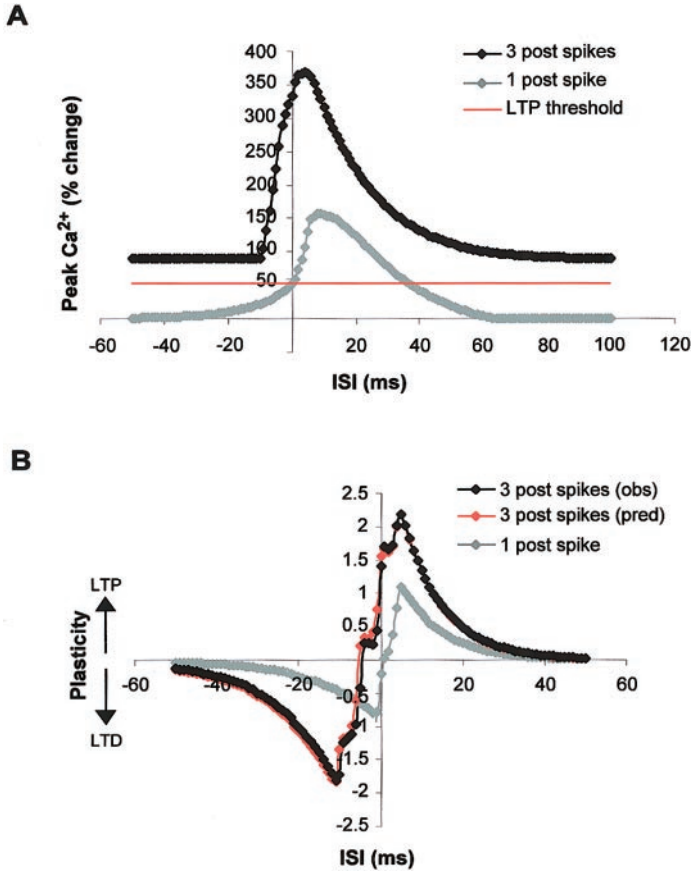

FIG. 4. Results from extending the induction protocols for *models 1* and *2*. A single presynaptic spike was paired with a burst of 3 postsynaptic spikes across a range of ISIs. *A*: percentage change in peak Ca^{2+} vs. ISI output of *model 1* for the single-spike (gray trace) and burst (black trace) protocols. Increasing the postsynaptic activity changes the shape and timing sensitivity of the function, and also shifts it entirely above the long-term potentiation (LTP) threshold (red line). *B*: STDP vs. ISI curves from *model 2* for the single spike pairings (gray) and burst (black) pairings. The red trace is the predicted STDP function for the burst protocol.

DISCUSSION

The purpose of these models was to determine whether the temporal properties of STDP can be accounted for by the standard LTP/LTD model, or whether STDP is more consistent with a mechanism that relies on two coincidence detectors.

Model 1

Our first simulations were based on the standard model, in which there is a single association point, and the degree of Ca^{2+} influx determines the transition between LTD and LTP. To produce the timing of LTD at negative ISIs, we assumed that postsynaptic spikes exhibit an afterdepolarization that partially depolarizes the membrane for tens of milliseconds. While the NMDAR is responsible for "recognizing" input order, Ca^{2+} from VGCCs enhances the graded response to post-pre activity across negative ISIs, thereby increasing the range of moderate Ca^{2+} concentrations that can produce LTD. Voltage-gated Ca^{2+} also acts to magnify the large Ca^{2+} increase after 0 ms that produces LTP. The contribution of voltage-gated Ca^{2+} to the central Ca^{2+} pool is supported by data showing that STDP relies on activation of both NMDARs and VGCCs (Bi and Poo 1998).

The NMDAR dissociation constant used in *model 1* was artificially short to produce a narrow range of ISIs that cause LTP. This is because there are little data indicating what might be constraining LTP to a limited range of positive ISIs given the duration of time that glutamate is bound to the NMDAR. We have, however, shown that while longer, more physiological constants result in LTP at a disproportionally long range of ISIs, they still produce the same type of plasticity profile (Fig. 2*D*).

The most significant result from *model 1* is that LTD occurs at long positive intervals. This is due to the drop in Ca^{2+} influx below the LTP threshold as the durations of the positive ISIs increase. A temporal profile of the shape shown from *model 1* in Fig. 2*D* is general to models that rely on a single coincidence detector coupled with the assumptions of the standard model. For example, models that did not include a VGCC contribution and relied only on Ca^{2+} from NMDA channels (data not shown) also produce LTD at positive intervals. In conclusion, since the standard model explicitly relies on increases in Ca^{2+} from a single source to generate LTD and LTP, and since longer and longer positive ISIs induce monotonically decreasing levels of Ca^{2+}, Ca^{2+} will eventually fall into the same range that produced LTD for negative ISIs. Thus our results do not depend on model parameters or the level of detail incorporated into the simulations.

Interestingly, our simulations account for recent experimental results in acute hippocampal slices in which LTD was obtained at negative and positive ISIs (Nishiyma et al. 2000). We predict that LTD in this case relies on the standard model via the same mechanisms that produce LTD by pairing presynaptic activity with postsynaptic depolarization to −40 mV (Cummings et al. 1996).

Model 2

Model 2, which incorporated a second coincidence detector, was more effective than *model 1* in simulating the observed relationship between plasticity and ISI reported in hippocampal

cell and slice cultures, and retino-tectal and cortical synapses (Bi and Poo 1998; Debanne et al. 1998; Feldman 2000; Zhang et al. 1998). In this model, the LTD and LTP components of STDP are detected and implemented by separate mechanisms. The effective LTP window relies on the time constant of the NMDAR-mediated component of the EPSP. The LTD window relies on the time constant of voltage-gated Ca^{2+} decay, as that is the persistent signal of postsynaptic activity for the second coincidence detector once it is activated by presynaptic input.

The major prediction of this model is that a second coincidence detector is required. In principle other molecules involved in the Ca^{2+} pathway, or a more complex model of the NMDA receptor (Senn et al. 2000; see following text) could fulfill this role. However, given the available experimental data, we would suggest that the mGluR pathway is the most likely candidate for the second coincidence detector. It is known that an mGluR-dependent form of homosynaptic LTD can be induced via LFS in the hippocampus (Huber et al. 2000; Oliet et al. 1997). There is also direct evidence from the work of Normann et al. (2000) showing that spike-timing dependent LTD in the hippocampus can be blocked by mGluR antagonists. Additionally, it is known that second-messenger systems activated by mGluRs function as a coincidence detector in Purkinje cells (Daniel et al. 1998). In a mechanism functionally similar to *model 2*, Ca^{2+} from VGCCs is coupled with a downstream product of the mGluR pathway diacylglycerol (DAG) in activating protein kinase C to produce LTD. Therefore, although the metabotropic pathway is relatively slow, there is evidence that it can produce temporal accuracy given the regulation of Ca^{2+} through VGCCs.

It is important to note that the model is *not* sensitive to the specific shape of the action potential, nor is it affected by small changes in the relative size of the EPSP, both of which could vary from cell to cell. In this aspect, it is more physiologically robust than *model 1*.

We cannot make predictions about which specific pathways are involved in STDP. For example, we cannot rule out the possibility that mGluRs have a modulatory or additive role in *model 1*, as suggested by Nishiyama et al. (2000). Additionally, *model 1* is consistent with experimental data showing that APV blocks the induction of LTD at negative ISIs (Bi and Poo 1998; Debanne et al. 1994; Feldman 2000). APV could affect spike timing LTD produced by the mechanisms in *model 2* since Ca^{2+} from NMDA channels could have a gating or modulatory effect. However, the model provides no explicit role for NMDAR activity in depression. Thus our mechanistic predictions are limited to the number of coincidence detectors involved.

Alternate STDP models

We examined alternate models for STDP as well. One possibility based on a single coincidence detector is that LTD is produced by effective decreases in Ca^{2+} influx below that caused by an EPSP or action potential alone. By this mechanism, if the postsynaptic cell shows an afterhyperpolarization, a post-pre pairing will decrease the EPSP and actually produce less calcium than baseline. However, this concept is not well supported by experimental observations.

One could also construct a single coincidence detector model with mechanisms that discriminate between the same calcium concentration at a negative and positive ISI. This would require an additional signal that could be used to mark or differentiate the order of the inputs. Alternatively, one could hypothesize that the NMDAR exhibits two functional states, one conducive to potentiation and one to depression (Senn et al. 2000). Both types of models are conceptually equivalent to our *model 2* in that they require two independent coincidence detectors.

Computational implications

Functionally LTD and LTP are thought to allow neurons to develop selective responses to correlated patterns of activity. Within this framework it has been hypothesized that STDP provides a way to implement synaptic competition (Song et al. 2000), or that STDP-like rules account for the development of responses to temporal order of stimuli (Abbott and Blum 1996). When considering the computational role of STDP, it is necessary to understand the following: *1*) how STDP generalizes from the single discrete pre- and postsynaptic spikes to more complex sequences and bursts and *2*) whether net plasticity in these cases can be predicted from the linear summation of the STDP functions observed experimentally.

Our results from *model 1* suggest that models relying on the same single pool of Ca^{2+} to produce LTD and LTP will generate an STDP function that is sensitive to spike properties and the induction protocol used (Fig. 4*A*). This sensitivity may be inherent in any mechanism relying only on NMDARs. Consequently, *model 1* may not be robust under physiological conditions in which spike shape varies or membrane potential fluctuates. In contrast, the existence of a metabotropic pathway to induce LTD (Normann et al. 2000; Oliet et al. 1997) could allow cells to independently measure the degree of LTD and LTP produced by complex sequences, and then compute the net plasticity. As shown in *model 2*, the presence of two coincidence detectors allows for stable plasticity-ISI functions. The increase in postsynaptic activity suggests an extension of the functional window that produces LTD. This is supported by observations in organotypic hippocampal slices in which the duration of the postsynaptic depolarization is varied (Debanne et al. 1994). Changing the postsynaptic activity to a burst of spikes in *model 2* produces plasticity that can be relatively well predicted from the single spike plasticity versus ISI function (Fig. 4*B*). However, this is largely due to the assumption that the LTD and LTP paths add linearly. Indeed, we believe that this is unlikely in vivo, and predict that the STDP function as a whole will undergo significant changes when pre- and postsynaptic parameters are varied.

Conclusions

Based on the results of our models, we propose that two types of STDP have been observed experimentally. The simulations we have described show that the first type, based on the standard Ca^{2+}-NMDAR model can generate temporally sensitive plasticity but generates LTD at long positive ISIs (as seen in Nishiyama et al. 2000). Additionally, we predict that STDP relying on the standard model will be sensitive to parameters such as shape of the action potential and initial EPSP amplitude.

Our data suggest that the second type of STDP, which is

strictly order-specific, producing LTD only at negative intervals, relies on the presence of two coincidence detectors. This mechanism is more robust and should not be qualitatively affected by variations in the action potential shape or EPSP amplitude. In fact, given the dual pathway nature of the model, LTD and LTP may be dissociable under certain experimental conditions. The model also predicts that induction protocols that use postsynaptic bursts should extend the range of ISIs that produce plasticity, but not affect the order specificity of the STDP, nor the ability to induce LTD (Debanne et al. 1994). Given these properties, this type of STDP is more likely to be of functional relevance for the complex spike patterns observed in vivo, and thus it will be of importance to characterize the nature of the second coincidence detector.

We thank Dr. Tom O'Dell and C. Marder for comments on earlier versions of this manuscript.

This research was supported by the Sloan and EJLB foundations, the National Science Foundation, and the Department of Defense (National Defense Science and Engineering Graduate Fellowship).

REFERENCES

ABBOTT LF AND BLUM KI. Functional significance of long-term potentiation for sequence learning and prediction. *Cereb Cortex* 6: 406–416, 1996.

BEAR MF AND ABRAHAM WC. Long-term depression in the hippocampus. *Annu Rev Neurosci* 19: 437–462, 1996.

BEKKERS JM AND STEVENS CF. NMDA receptors at excitatory synapses in the hippocampus: test of a theory of magnesium block. *Neurosci Lett* 156: 73–77, 1993.

BI Q-G AND POO M-M. Synaptic modifications in cultured hippocampal neurons: dependence on spike timing, synaptic strength, and postsynaptic cell type. *J Neurosci* 18: 10464–10472, 1998.

BUONOMANO DV. Decoding temporal information. A model based on short-term synaptic plasticity. *J Neurosci* 20: 1129–1141, 2000.

CUMMINGS JA, MULKEY RM, NICOLL RA, AND MALENKA RC. Ca^{2+} signaling requirements for long-term depression in the hippocampus. *Neuron* 16: 825–833, 1996.

DANIEL H, LEVENES C, AND CRÉPEL F. Cellular mechanisms of cerebellar LTD. *Trends Neurosci* 21: 401–407, 1998.

DEBANNE D, GAHWILER BH, AND THOMPSON SM. Asynchronous presynaptic and postsynaptic activity induces associative long-term depression in area CA1 of the rat hippocampus in vitro. *Proc Natl Acad Sci USA* 91: 1148–1152, 1994.

DEBANNE D, GAHWILER BH, AND THOMPSON SM. Long-term synaptic plasticity between pairs of individual CA3 pyramidal cells in rat hippocampal slice cultures. *J Physiol (Lond)* 507: 237–247, 1998.

FELDMAN DE. Timing-based LTP and LTD at vertical inputs to Layer II/III pyramidal cells in rat barrel cortex. *Neuron* 27: 45–56, 2000.

HINES ML AND MOORE JW. Computer simulations with NEURON. http://neuron.duke.edu/1997.

HUBER KM, KAYSER MS AND BEAR MF. Role for rapid dendritic protein synthesis in hippocampal mGluR-dependent long-term depression. *Science* 288: 1254–1257, 2000.

LESTER RAJ AND JAHR CE. NMDA channel behavior depends on agonist affinity. *J Neurosci* 12: 635–643, 1992.

LEVY WB AND STEWARD O. Temporal contiguity requirements for long-term associative potentiation/depression in the hippocampus. *Neuroscience* 8: 791–797, 1983.

LISMAN J. A mechanism for the Hebb and the anti-Hebb processes underlying learning and memory. *Proc Natl Acad Sci USA* 86: 9574–9578, 1989.

MARKRAM H, LUBKE J, FROTSCHER M, AND SAKMANN B. Regulation of synaptic efficacy by coincidence of postsynaptic APs and EPSPs. *Science* 275: 213–215, 1997.

NISHIYAMA M, HONG K, MIKOSHIBA K, POO M-M, AND KATO K. Calcium stores regulate the polarity and input specificity of synaptic modification. *Nature* 408: 584–588, 2000.

NORMANN C, PECKYS D, SCHULZE CH, WALDEN J, JONAS P, AND BISCHOFBERGER J. Associative long-term depression in the hippocampus is dependent on postsynaptic N-type Ca^{2+} channels. *J Neurosci* 20: 8290–8297, 2000.

OLIET S, MALENKA RC, AND NICOLL RA. Two distinct forms of long-term depression coexist in CA1 hippocampal pyramidal cells. *Neuron* 18: 969–982, 1997.

SENN W, MARKRAM H, AND TSODYKS M. An algorithm for modifying neurotransmitter release probability based on pre- and postsynaptic spike timing. *Neural Comput* 13: 35–67, 2000.

SONG S, MILLER KD, AND ABBOTT LF. Competitive Hebbian learning through spike-timing-dependent synaptic plasticity. *Nature Neurosci* 3: 919–926, 2000.

ZHANG LI, HUIZHONG WT, HOLT CE, AND POO M-M. A critical window for cooperation and competition among developing retinotectal synapses. *Nature* 395: 37–44, 1998.